Modeling and Simulation of Integrated Luminescence Detection Platforms

Khaled Salama*[a], Helmy Eltoukhy[a], Arjang Hassibi[b] and Abbas El Gamal[a]

[a]Information Systems Laboratory (ISL), Stanford University, Stanford, CA USA 94305
[b]Center for Integrated Systems (CIS), Stanford University, Stanford, CA USA 94305

ABSTRACT

We developed a simulation model of an integrated CMOS-based imaging platform for use with bioluminescent DNA microarrays. We formulate the complete kinetic model of ATP based assays and luciferase label-based assays. The model first calculates the number of photons generated per unit time, i.e., photon flux, based upon the kinetics of the light generation process of luminescence probes. The photon flux coupled with the system geometry is then used to calculate the number of photons incident on the photodetector plane. Subsequently the characteristics of the imaging array including the photodetector spectral response, its dark current density, and the sensor conversion gain are incorporated. The model also takes into account different noise sources including shot noise, reset noise, readout noise and fixed pattern noise. Finally, signal processing algorithms are applied to the image to enhance detection reliability and hence increase the overall system throughput. We will present simulations and preliminary experimental results.

Keywords: Luminescence probes, Modeling, CMOS sensor, post-processing

1. INTRODUCTION

Conventional biological assays are highly repetitive, labor intensive and are performed with microliter volume samples. The associated biochemical procedures comprising these protocols often require days or weeks to perform at a cost of hundreds of dollars per test. There is a basic interest in the development of inexpensive techniques and portable biosensors for environmental and biomedical diagnostics. Of interest is developing new techniques and sensors, not only to selectively identify target compounds, but also to assay large numbers of samples. Problems remain in detecting and quantification of low levels of biological compounds reliably, conveniently, safely and quickly. A simplified system for biochemical testing can be divided into four steps: sample preparation, assay, detection and data analysis as shown in Figure 1.

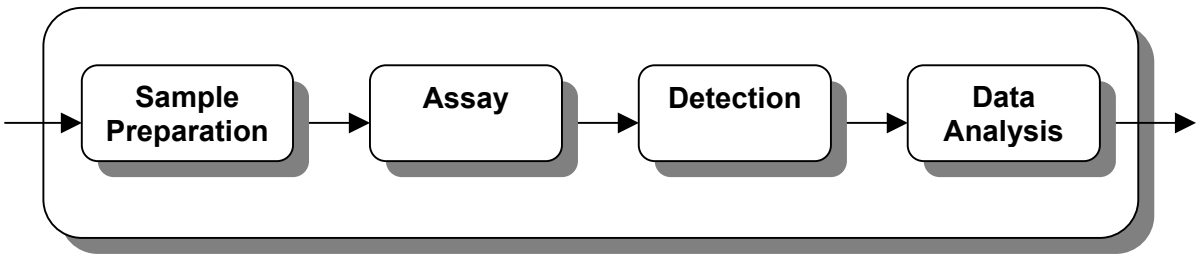

Figure 1: General system currently used for biochemical testing.

Despite efforts to develop chips for biological assay detection, there continues to be a need to improve implementations of micro-scale detection and processing systems for further convenience and portability. Furthermore, there continues to be a need for designs that accommodate efficient integrated circuit manufacturing techniques to realize associated cost savings. Currently, each step is being separately automated and miniaturized. In order to further increase throughput and reduce cost, we propose the integration of three of these four steps into a single miniaturized platform as shown Figure 2.

*ksalama@stanford.edu; phone 1 650 725 9696; fax 1 650 724 3648

Microarrays and Combinatorial Technologies for Biomedical Applications: Design, Fabrication, and Analysis, Dan V. Nicolau, Ramesh Raghavachari, Editors, Proceedings of SPIE Vol. 4966 (2003) © 2003 SPIE · 1605-7422/03/$15.00

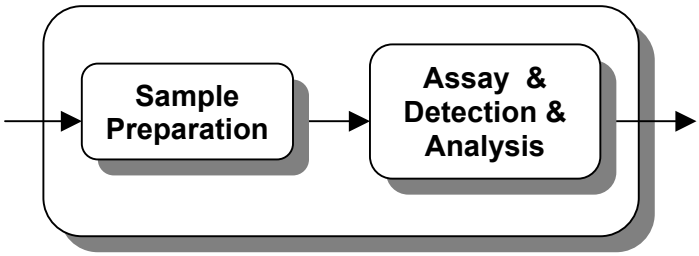

Figure 2: Proposed system for future biochemical testing.

A variety of sensing schemes have been developed for molecular detection, such as electrochemical, optical absorption, interferometric sensing, luminescence and fluorescence sensing. In this paper we focused on *luminescence sensing*. Nowadays, commercially available platforms for photon detection use bulky CCD camera-based setups. However, due to the light loss in the optical path and the limited chip integration capabilities of CCDs, these systems are not well suited to such applications. As standard Complementary Metal-Oxide-Semiconductor (CMOS) technology scales down to the sub-micron regime, CMOS image sensors are emerging as a viable alternative to CCDs, especially for low power and embedded applications. We investigated the design of an integrated CMOS-based imaging platform for use with bioluminescent microarrays. Existing silicon-based CMOS technology makes it possible to integrate photodetectors, conditioning circuits, and digital signal processing functions on a single chip, potentially providing low cost, low power integrated biological testing platforms. However, in a highly miniaturized biological testing system, such as for DNA sequencing, the photogenerated signals can be very weak and it is not clear that a CMOS based system would have high enough sensitivity and low enough noise to reliably perform the detection. Assessment is performed by modeling current CMOS process information in addition to the use of circuit and sensor simulators. Through such simulations, the noise and the sensitivity of the system can be quantified leading to accurate estimation of assay density and throughput limits.

Initially we describe the general kinetics of the light generation process of luminescent probes and formulate the complete kinetic model of ATP based assays, luciferase label-based assays and pyrosequencing, a label-independent bioluminescent method of short run DNA sequencing that utilizes luciferase (firefly enzyme) to generate photons upon correct incorporation of nucleotide base pairs onto the strand to be sequenced. The photon flux coupled with the system geometry is then used to calculate the number of photons incident on the photodetector plane. Subsequently the characteristics of the imaging array including the photodetector spectral response, its dark current density, and the sensor conversion gain are incorporated. The model also takes into account different noise sources including shot noise, reset noise, readout noise and fixed pattern noise. Finally, signal processing algorithms are applied to the image to enhance detection reliability and hence increase the overall system throughput. Microarray imaging techniques typically suffer from cross-talk generated from adjacent assays. To ameliorate such effects, linear minimum mean square error equalization is used since it minimizes noise amplification and is relatively easy to implement in software or hardware.

The rest of the paper is organized as follows. In section 2, we describe the light generation process. In section 3 we describe the sensor model. In section 4 we present preliminary simulation and experimental results.

2. LUMINESCENCE LIGHT GENERATION PROCESSES

Luminescence assay techniques can be divided into two general categories. The first category is termed, direct target detection, in which the photon emitting species physically interacts with the target of interest and the coordinates where the light is generated is of the target-probe complex. An example of this approach is luminescence based immunoassays which usually involve probing a protein of interest with a primary antibody that reacts with a secondary antibody. Light is produced when a luminescence probe is acted upon by the enzyme, which is bound, to the secondary antibody. The second category is termed, indirect or linked detection method, in which the luminescent species indirectly measures the targeted characteristic, usually through an intermediate chemical process[1-5].

It is imperative to realize that multiplexed assays are only feasible in the direct luminescence approach, where the targeted molecules and light generation source (the probe) are localized in identical coordinates (e.g. microarray assays[6]). On the contrary in the indirect methods it is challenging to confine the photon generation process and have multiplexed assays, since the light generating species diffuse through the reaction medium. Consequently in practice the reaction medium of different targets is individually isolated.

2.1 Luminescence light generation

The light generation from a typical luminescence process is a function of chemical reaction kinetics which generates photons as a function of time. The rate of a reaction, in general, is the speed at which reactants are converted into products. From the Gibbs free energy of a reaction, one can predict the direction in which a chemical change will take place and the amount of energy consumed/evolved. If we consider the scenario where enzyme species E (the catalyst), converts the substrate molecule S into product P then the stoichiometric formula for this process is

$$S + E \xleftrightarrow{k_f, k_r} E + P, \tag{1}$$

where k_f and k_r are the association and disassociation rate constants. In (1) the reaction rate can be defined as

$$rate = \frac{d[P]}{dt} = -\frac{d[S]}{dt} = k_f[S][E] - k_r[E][P], \tag{2}$$

where $[E]$, $[S]$ and $[P]$ are the concentrations of the enzyme, substrate and product in the medium respectively. Now if suppose that the above process is a luminescence enzymatic reaction, with quantum yield (QE) of α, then the photon generation rate I in volume V of the reaction medium is (A is the Avogadro number)

$$I = (\alpha VA)\frac{d[P]}{dt} = (\alpha VA)\cdot[E]\cdot\left(k_f[S] - k_r[P]\right), \tag{3}$$

and the total number of photons generated by this luminescence process N_{ph}, in an arbitrary time interval T is

$$N_{ph} = (\alpha VA)\cdot[E]\cdot\int_T \left(k_f[S] - k_r[P]\right)\cdot dt. \tag{4}$$

It is important to understand that the rate constants of the reaction are not always concentration independent, and generally when we extensively increase the amount of relevant species in the reaction medium, it reaches a maximum value (saturation concentration).

In luminescence assays the experiment is typically setup in such a way that the luminescence probe (e.g. a light generating enzyme) either reports the quantity of a substrate molecule (e.g. ATP), or the molecule which it binds to (e.g. luciferase-based labels in immunoassays). The photon generation rate from the luminescence reaction, which is a function of target concentration, is then measured, and correlated to the target concentration.

2.1.1 Substrate detection kinetics

In the first group of luminescence assays, the rate at which photons are generated represents the substrate concentration (3), and as the substrate is consumed by the catalyst the light intensity decreases. This results in an assay in which the kinetics measurement of the light is information bearing and the emission rate will eventually become zero. If we assume that the disassociation rate is negligible light intensity for such as assay with initial substrate concentration $[S_0]$ is

$$I(t) = (\alpha VA)\cdot\frac{d[P(t)]}{dt} = (\alpha VA)\cdot k_f[E][S_0]\cdot e^{-k_f[E]t}, \tag{5}$$

and the total amount of photons form time $t = 0$, the start of the process, to $t = T$ is

$$N_{ph} = (\alpha VA) \cdot [S_0] \cdot (1 - e^{-k_f [E] T}) . \quad (6)$$

As we can see the photon intensity is proportional to the target concentration (substrate), but the light intensity decays exponentially with a time constant which is a function of catalyst concentration and turnover rate k_f. In this system the total number of photons generated as a function of time is less than or equal to the substrate present in the medium and as integration time becomes infinite,

$$N_{ph-total} = (\alpha VA) \cdot [S_0] . \quad (7)$$

2.1.2 Catalyst detection kinetics

The second approach in luminescence assays is to link the target molecule quantity to a luminescence catalyst. In this methodology generally the substrate is provided such that it is above the saturation level of the process, therefore its consumption has little effect on the reaction kinetics. If the saturation concentration for the substrate is $[S_{\max}]$, and the target concentration is equal to the catalyst $[E]$, the light intensity becomes

$$I(t) = (\alpha VA) \cdot \frac{d[P(t)]}{dt} = (\alpha VA) \cdot k_f [S_{\max}][E] . \quad (8)$$

The light intensity based on (8) is independent of time, and is a linear function of the target (or the catalyst) concentration, thus the total number of photons generated from this process in fact becomes a function of integration time,

$$N_{ph} = (\alpha VA) \cdot k_f [S_{\max}][E] \cdot T . \quad (9)$$

Although the number of target molecules might be very small (low $[E]$) in these assays, because the light intensity is steady, one can have long integration times to collect a significant number of photons. These type of assays usually have very high sensitivity and their dynamic range is also controllable by adjusting the integration time.

2.2 Example models of luminescent assays

The two basic models of luminescence detection methodologies formulated in the previous section, can be in fact applied to a variety of currently used assays. As examples in this paper we initially study ATP bioluminescent assays where adenosine 5′-triphosphate (ATP) quantity in the sample is estimated. The next assay is where the luminescent enzyme is a label of the target, and the last system is Pyrosequencing which is an enzymatic system for DNA sequencing using luciferase-luciferin bioluminescent complex.

2.2.1 ATP measurement assays

ATP bioluminescent assays are designed to measure the quantity of adenosine 5′-triphosphate (ATP) in the sample[7]. ATP assay quantification applications include indirect measurement of bacteria, yeasts, fungi and other microorganisms, which have regulated number of ATP, in foodstuffs, beverages, water, woodpulp, cosmetics and other mediums. The assay uses recombinant luciferase to catalyze the following reaction.

$$ATP + luciferin + O_2 \xrightarrow{Lucferase} AMP + oxyluciferin + CO_2 + PPi + h\nu . \quad (9)$$

In most practical applications the concentration of luciferin is high enough that we can consider it to be in deep saturation as shown in Figure 3(a). In this case the rate of ATP consumption is

$$\frac{d[ATP]}{dt} = -k_L [E][luciferin_{\max}][ATP_0] \cdot e^{-k_f [E][luciferin_{mac}] t} , \quad (10)$$

where k_L is the association rate of the macro-reaction. As we can see in (10) $k_t = k_L \cdot [E][luciferin_{\max}]$ is a constant and therefore we introduce k_t as the turnover rate of the ATP consumption in this assay, and the photon generation rate becomes

$$I(t) = (\alpha VA) \cdot k_t \cdot [ATP_0] \cdot e^{-k_t t} \tag{10}$$

The quantum efficiency of the luciferase is about 0.88, and the turnover rate of the enzyme, depending the ratio of luciferase to the ATP, can vary from 0.1 to 1 sec^{-1} (glow compared to flash)[8]. Now for the glow process, the light intensity is

$$I(t) \approx 5.3 \times 10^{22} V[ATP_0] \cdot e^{-0.1t}. \tag{11}$$

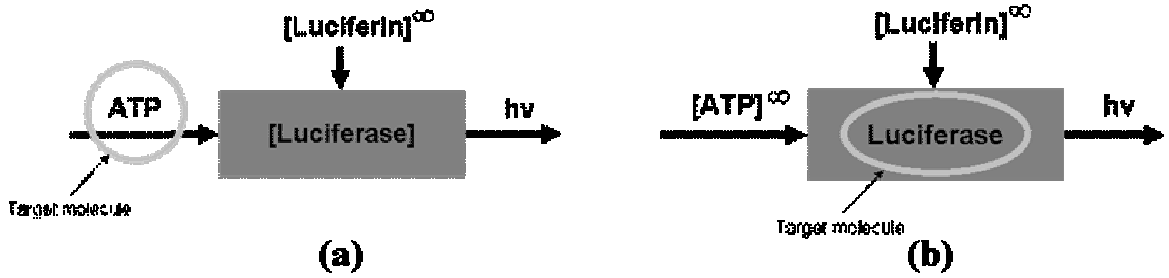

Figure 3: Block diagram of (a) ATP detection assay, and (b) Luciferase detection system. The ∞ symbol corresponds to excess substrate concentration.

2.2.2 Luminescent labels

If the reporter of a specific biological process is the catalyst of a luminescence reaction, then the assay can be optimized in such a way that the rate limiting factor becomes the catalyst concentration[7]. In such an assay any change in target concentration changes the catalyst concentration, therefore alters the photon flux intensity as shown in Figure 3(b). The light intensity in the case where luciferase is the label of the target is

$$I(t) \approx 5.3 \times 10^{22} V[E_0], \tag{12}$$

and the total number of photons accumulated in time interval T is defined by

$$N_{ph} \approx 5.3 \times 10^{22} V[E_0] \cdot T. \tag{13}$$

2.2.3 Pyrosequencing

Pyrosequencing is based on the detection of released pyrophosphate during DNA synthesis. In the cascade of enzymatic reaction, visible light is generated that is proportional to the number of incorporated nucleotides[9,10]. The cascade starts with a DNA polymerization reaction in which inorganic pyrophosphate (PPi) is released as a result of nucleotide incorporation by polymerase. The released PPi is subsequently converted to ATP by ATP sulfurylase. The synthesized ATP provides the energy for luciferase to generate photons. Unincorporated deoxy-nucleotides and ATP are degraded by the enzyme apyrase to reset the enzymatic system after the incorporation test. The enzymatic reactions in this method are

$$(DNA)_{n+1} + dNTP \xrightarrow{Polymerase} (DNA)_{n+1} + PPi \tag{14}$$

$$PPi + APS \xleftarrow{ATP-Sulfurylase} ATP + SO_4^{-2} \tag{15}$$

$$ATP + luciferin + O_2 \xrightarrow{Lucferase} AMP + oxyluciferin + CO_2 + PPi + h\nu \tag{16}$$

$$dNTP \xrightarrow{Apyrase} dNMP + 2Pi\,, \tag{17}$$

where APS is adenosine phosphosulfate, AMP is adenosine monophosphate, dNTP is deoxynucleotide triphosphate, and Pi is phosphate. As shown in Figure 4 this enzymatic system regulates the light generation by recycling PPi, but the degrading enzyme, apyrase, breaks all nucleotide and ATP molecules in time, therefore decreases the light intensity. If we assume that PPi regulation has a unity gain positive feedback, and the turnover rate of apyrase is k_a then the light generated by single incorporation from this bioluminometric assay is

$$I(t) = (\alpha VA) \cdot k_t \cdot [DNA] \cdot e^{-k_a t} \tag{18}$$

For most practical applications, $k_a \approx 0.05\,\mathrm{sec}^{-1}$ and $k_t \approx 1\,\mathrm{sec}^{-1}$, consequently the light intensity becomes

$$I(t) = 5.3\times 10^{23} \cdot V[DNA] \cdot e^{-0.05t} \tag{19}$$

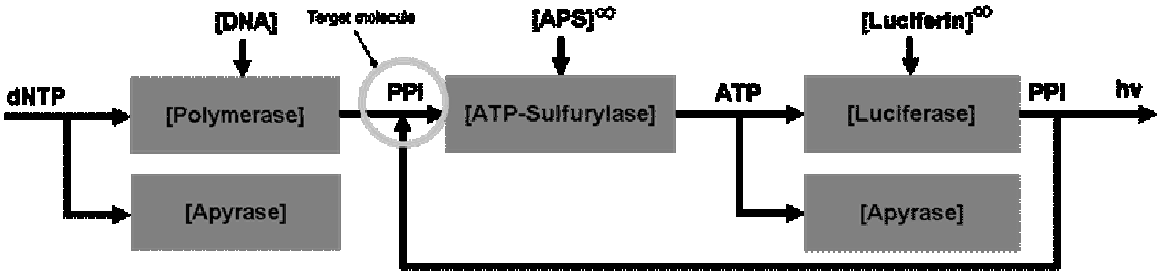

Figure 4: Block diagram of Pyrosequencing where PPi release from DNA polymerization is measured. The ∞ symbol corresponds to excess concentration.

3. INTEGRATED LUMINESCENCE DETECTION PLATFORM

Having established a general model for the quantum efficiency of bioluminometric assays, we can now focus our attention upon the detection portion of the overall system. Detection is currently performed using CCD-based imaging systems. A charge-coupled device (CCD) is an analog charge shift register. A CCD image sensor comprises an array of photodetectors, typically photodiodes, which convert light into charge and uses the CCDs for shifting out the collected charge. CCDs are fabricated in a nonstandard semiconductor process that is solely optimized for sensing and charge transfer[11]. As a result, CCD image sensors can achieve very high sensitivity (in V/lux.s), low noise, and low non-uniformity. This, however, requires the use of several high supply voltages resulting in high power consumption. Moreover, no other analog or digital circuits, such as for clock generation, timing, analog to digital (A/D) conversion, digital processing and storage, can be integrated with a CCD image sensor on a single chip resulting in multi-chip imaging system implementations with high power consumption, high cost, and large size. CMOS technology, by comparison, provides unlimited flexibility and integration possibilities[12]. In a CMOS technology, sensor readout can be non-destructive allowing for multiple read-outs during exposure for enhancing signal-to-noise ratio and dynamic range. CMOS technology also provides unlimited potential for customizing photodetector sizes and shapes and the readout architecture to meet the needs of specialized applications.

3.1 System Description

Current technologies employ sensors that are relatively far removed from the target assay due to intermediary optics, hence failing to capture a significant portion of generated light. We propose to couple both the sensor array and the

biological assay reaction as shown in Figure 5(a). The proximity of the target assays to the proposed system will obviate a large portion of such light loss, which can increase signal-to-noise ratio and/or allow for decreased biological sample size, a necessary requirement for further miniaturization[13]. A possible implementation of the proposed CMOS image sensor platform is shown in Figure 5(b). It consists of a 2D array of pixels, each containing a photodetector and transistors for readout. The collected charge is read out in a manner similar to a digital memory using row/column address decoders and column amplifiers. The system includes column level analog-to-digital converters to convert the collected charge into a digital format that is stored in on-chip frame memory. A dedicated digital signal processor (DSP) is integrated on the chip to perform the needed computations. It also includes a control unit that synchronizes the operation of the entire chip and the flow of information between the different blocks.

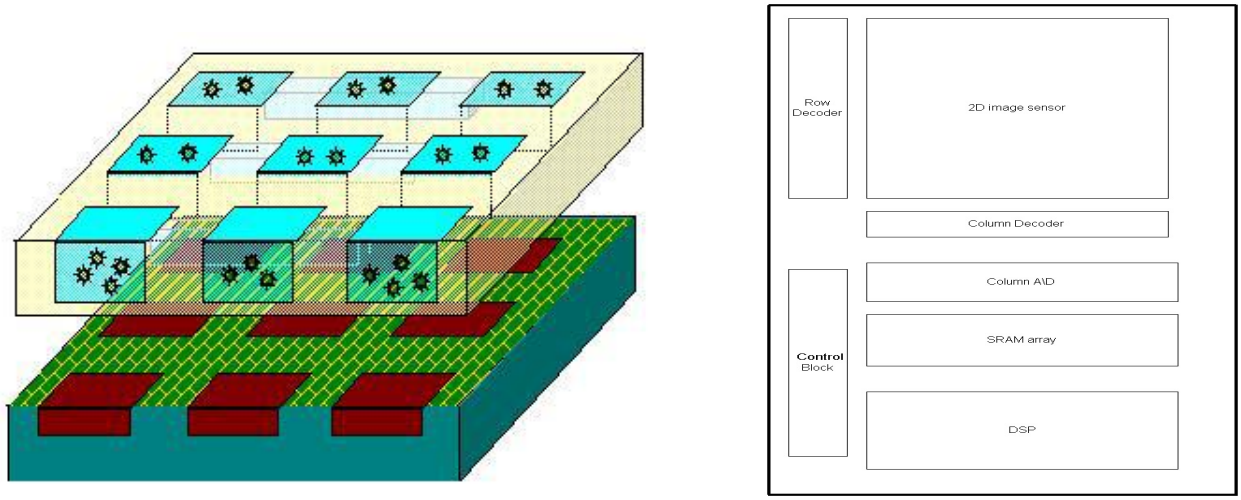

Figure 5: (a) Schematic of the tight coupling between the sensor array and the biological assay reactions, (b) Sensor block diagram showing the major components (2D photodetector array, Column A\D, SRAM array, DSP)

During readout, the electrical voltage is sensed using the Row Decoder. The Row Decoder is used to generate a Word signal to activate a single row while the voltage generated at the pixel is read through the Bit line using the Column Amplifier. The Column Decoder is used to select the specific column (*i.e.*, pixel) to be read. The output is then transferred for further processing. In a CMOS technology, sensor readout can be non-destructive, thereby allowing for multiple read-outs during exposure; read-outs that can be utilized for enhancing signal-to-noise ratio and dynamic range at both the high and low illumination ends. Furthermore, these multiple frames can be obtained with only one reset noise added to the signal[14].

A key feature of the system is the integration of the A/D blocks on the chip. This allows the analog signal read to be transformed into a digital format that is easy to store and process. The proposed system includes memory that is used to store multiple frames. The proposed system can operate in two different modes, snapshot and multi- capture. In snapshot mode, a single image is captured per test sample. This mode tends to improve the signal-to-noise ratio of the output making use of the increased signal captured. It also provides low power operation since it involves running different parts of the chip, such as A/D conversion, only once. In the multi-capture mode, several non-destructive reads of the signal are performed while the incident light is being collected. This is mainly facilitated by the high speed capability of CMOS technology as compared with other imaging technologies. As mentioned, this unique feature allows the capturing of several images while suffering from only a single reset noise addition. CCDs, on the other hand, add reset noise for each image captured. Moreover, this mode, coupled with subsequent on-chip signal processing, can actually improve the signal-to-noise ratio of the captured data and consequently increase system post-detection analysis accuracy[15].

3.2 Optics Model

Conventional CCD-based imaging systems employ intermediary optics in order to focus the collected light onto the sensor plane. For microscopy applications, resolution is important for feature discrimination; however, for luminescence applications the collection and quantification of generated photons takes precedence. This implies that we can indeed forego with conventional optics and couple the luminescent assays directly to the sensor plane. In order to assess the gain in light collection through the dispensation of optics, we can employ geometric optics to calculate a first-order relation. Assuming we are imaging a point source located a distance, U, from the lens, we can approximate the numerical aperture, NA, of the object side of this setup as $\frac{D}{2U}$, where D is the diameter of the lens aperture and we are assuming air is the imaging media. The amount of light collected by the lens is proportional to the square of this result. Assuming typical numbers, D=0.5f and U = 2f, where f is the focal length, yields a light collection ability of only 1.6%. Clearly, there is the potential for large signal gains using the proposed scheme.

In order to better model the proposed scheme, we used an optical simulator and input the specific luminescent assay and sensor parameters of the proposed setup in order to derive the point spread function, PSF, of the signal sensed at the photodetector surface. Figure 6 shows both the modeled experimental setup and the simulated intensity distribution at the sensor plane. This information is used to optimize assay spacing and pixel design for maximizing SNR and reduction of crosstalk.

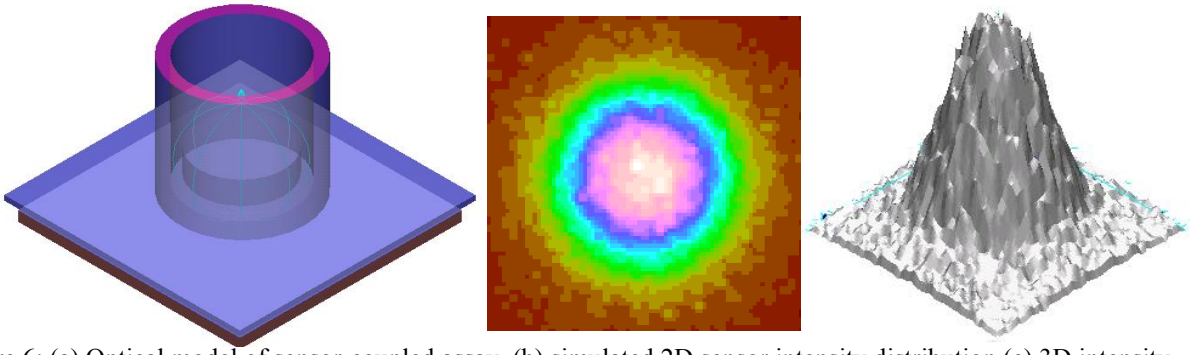

Figure 6: (a) Optical model of sensor-coupled assay (b) simulated 2D sensor intensity distribution (c) 3D intensity distribution

3.3 Sensor Model

Modeling of sensor parameters is necessary if maximization of the SNR of the photogenerated signal is to be achieved. Most visible light sensors comprise a 2D photodetector array, which is divided into pixels. Each pixel contains a photodiode shown in Figure 7(a). Photons incident on the photodiode are converted to electrical charge (Q), which is integrated over the diode capacitance (C_D). The amount of charge collected is proportional to the light intensity and it might be clipped by the well capacitance (Q_{max}) in high illumination. At the end of exposure time (t_{int}) the amount of charge is read as an electrical voltage signal (V_o).

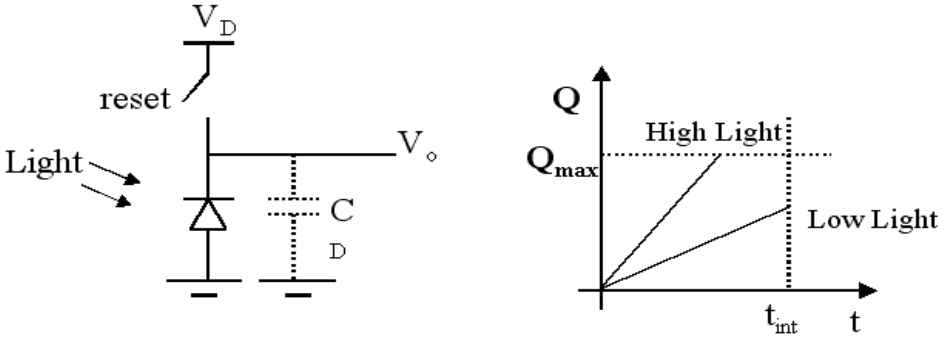

Figure 7: (a) Simplified photodiode pixel model , (b) photocharge Q(t) under different illumination conditions

During integration time, T_{int}, the photodiode integrates the incident light and generates a charge, Q, which is given by

$$Q = \frac{i_{ph} T_{\text{int}}}{q} \quad . \tag{20}$$

Several sources contribute to noise during the collection of the photogenerated signal. The shot noise generated during integration can be modeled as a Gaussian noise source with zero mean and variance, $\frac{1}{q}(i_{ph} + i_{dc})T_{\text{int}}$. Other sources include read noise and reset noise which are zero mean with variance, σ_r^2. The variance of the noise power can be easily calculated using

$$\sigma_n^2 = \frac{1}{q}(i_{ph} + i_{dc})T_{\text{int}} + \sigma_r^2 \tag{21}$$

The Signal-to-Noise Ratio, SNR, is defined as the ratio between the photogenerated signal power to the noise power and is given by

$$SNR = \frac{i_{ph}^2 T_{\text{int}}^2}{q^2(\frac{1}{q}(i_{ph} + i_{dc})T_{\text{int}} + \sigma_r^2)} \tag{22}$$

In order to achieve a relatively high SNR the integration time should be increased. At the same time the read noise variance, σ_r^2, should be minimized by using low noise circuits.

4. SIMULATION AND EXPERIMENTAL RESULTS

We built an isolated imaging chamber for pyrosequencing. The system employs an ultrasonic sprayer developed by us for nucleotide and enzyme delivery to the target assays above the imaging apparatus as shown in Figure 8. In order to simulate the types of conditions that would be encountered in an integrated CMOS system, a scientific-grade CCD imager is incorporated with the ultrasonic sprayer. This CCD imager is specially assembled without optics so as to allow direct placement of the assay slide onto the pixel array of the sensor. Using a bare CCD offers great opportunities for low signal level detection since more than 90% of the light can be lost due to the optical geometry. The CCD is connected to a dedicated PC for online processing of the image data. Also implemented, is an integrated software control program, which can operate the robotic arm of the sprayer and capture images simultaneously. This experimental setup allows for accurate measurement of the quantum efficiency of the reaction, which can be used to calculate optimal assay sizes and throughput limits.

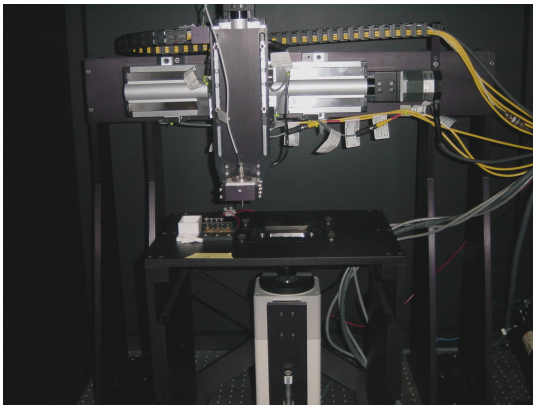

Figure 9: Image of the prototype system including a robot-arm, an ultrasonic sprayer and a cooled CCD sensor

As an example, the experimental system was used to measure the light intensity during the incorporation of a single base. Using 100 fmol of DNA per well and combined with signal processing, we measured peak signal-to-noise ratio of 750. Moreover, 100 fmol represents a tenfold decrease in the amounts currently used in commercial Pyrosequencing systems, and we were still able to reliably detect incorporation.

The final step in biochemical testing is information analysis. Here, the data from the assay is processed in order to achieve accurate detection. Currently, this processing is performed using a real time Matlab script running on the aforementioned PC. We implemented a simple but efficient algorithm for signal detection, which runs in parallel with the data acquisition software. The algorithm automatically performs background subtraction of noise and utilizes line binning to achieve higher signal to noise ratio. A low pass filter is utilized to smooth the resultant signal and remove any high frequency noise components. Also integrated with the script is a routine for reduction of crosstalk using the modeled system PSF. Figure 10 illustrates the output of the script for the case of two adjacent pyrosequencing assays.

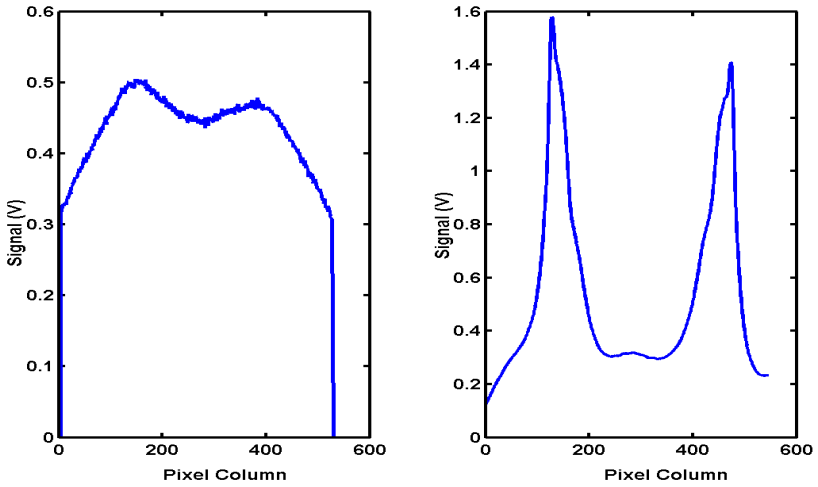

Figure 10: Plot of measured output signal voltage from each column of the CCD array for several 1 second intervals using 0.1pmol of DNA.

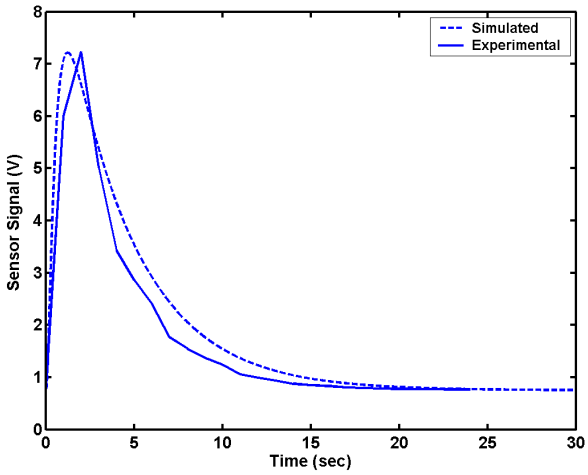

Figure 11: Experimental data versus combined chemistry and sensor simulation of detected signal versus time of nucleotide incorporation in a pyrosequencing reaction.

Using the collected experimental data to fine-tune the analytical models of the chemical kinetics, optics and photodetector array, we have designed a simulator for estimating the minimum number of photons needed from a bioluminometric assay to achieve an acceptable signal-to-noise ratio. For example, Figure 11 shows a plot of both the simulated and experimental signals generated in the CCD versus time during incorporation of one nucleotide in a pyrosequencing reaction using 100 fmol of DNA. As is readily seen, the analytical models are fairly well corroborated

by the experimental data. Furthermore, using typical parameter and CMOS process values at room temperature, our model predicts that 0.5 photon/sec/μm^2 in conjunction with T_{int} =10 sec and 100µm X 100µm diodes would be needed to achieve a signal-to-noise ratio of 10. This implies that an integrated luminescence detection system would be capable of performing pyrosequencing with as little as 1 fmol of DNA, an amount three orders of magnitude lower than the current state-of-the-art.

5. CONCLUSION

We developed a simulation model of an integrated CMOS-based imaging platform for use with bioluminescent DNA microarrays from the photon generation process to the final output data. We were able to assess the performance of a CMOS-based platform. We constructed a prototype system to verify experimentally the developed models. Using this experimental setup we are able to obtain accurate measurements of the quantum efficiency, temporal kinetics and spatial distribution of the reaction, which are used to calculate the optimal assay sizes and throughput limits for the CMOS-based system. We show that for pyrosequencing 100 femtomoles of DNA molecules with a significant increase in the signal-to-noise ratio can be reliably detected with our experimental system. Furthermore, analytical models of the overall system predict the envisioned platform will possess a detection limit of below 1 femtomole of DNA.

AKNOWLEDGMENT

The work reported in the paper is supported under the Programmable Digital Camera Program by Agilent, Canon, HP and Kodak. The authors wish to thank Prof. Ronald Davis, Dr. Mostafa Ronaghi, Dr. Peter Griffin and Ali Agah for their valuable insight and helpful discussions. We acknowledge the support of the Stanford Genome Technolgy Center in conducting most of the experimental work.

REFERENCES

1. K. Tang, D. Fu, S. Kotter, RJ Cotter, CR Cantor and H. Koster, "Matrix-assisted laser desorption/ionization mass spectrometry of immobilized duplex DNA probes", *Nucleic Acids Res*earch, **23**, 3126-3131
2. H. Koster, D. van den Boom, A. Braun, A. Jacob, C. Jurinke, DPLittle, and K. Tang, "DNA analysis by mass spectrometry: applications in DNA sequencing and DNA diagnostics", *Nucleosides & Nucleotides*, **16**,563-571, 1997.
3. A.J. de Mello, *Surface Analytical Technique for Probing Biomaterial Processes*, 1, CRC Press, Boca Raton, New York, 1996.
4. R. P Haugland, *Handbook of Fluorescent Probes and Research Chemicals*, Molecular Probes, Inc., Eugene, Oregan, 1998.
5. N. Van Dyke, C. Van Dyke and K. Woodfork, *Luminescence Biotechnology: Instruments and Applications*, 1, CEC Press, Boca Raton, New York, 1 2002.
6. M. Schena, D. Shalon, R. W. Davis and P.O. Brown, "Quantitative monitoring of gene expression patterns with a cDNA microarray", *Science,* **270**, 467-470, 1995.
7. L. J. Kricka,"Clinical and biological applications of luciferases and luciferins", *Anal. Biochem.,* **175**, 14-22, 1988.
8. L. Brovko, O. Gandel'man, T. Polenova and N. Ugarova, "Kinetics of Bioluminescence in the Firefly Luciferin-Luciferase System", *Biochem. (Moscow),* **59**, 195-201, 1994.
9. M. Ronaghi, S. Karamohamed, B. Pettersson, M. Uhlen and P. Nyren, "Real-Time DNA Sequencing Usind Detection of Pyrophosphate Release", *Anal. Biochem,,* **242**, 84-89.
10. M. Ronaghi, "Pyrosequencing Sheds Light on DNA Sequencing", *Genome Research*, **11**, 3-11, 2001.
11. G. Holst, *CCD Arrays, Cameras, and Displays*, Second Edition, *SPIE Press*, 1991.
12. Fossum, E. Active Pixel Sensors: are CCD's dinasours, *Proceedings of SPIE,* 1900:2-14,1993.
13. P. B. Griffin, Ali Agah, J.D. Plummer, H. Eltoukhy, K. Salama, A. El Gamal, M. Ronaghi and R.W. Davis, "Miniaturized DNA Analysis Devices", invited presentation at the First International Forum on Post-Genome Technology, Xian, China, April 19-20, 2002.
14. A. El Gamal, D. Yang and B. Fowler, "Pixel-level Processing – Why, What and How", *Proceedings of the SPIE – The International Society for Optical Engineering*, 5650, 2-13, 1999.
15. D. Yang, B. Fowler and A. El Gamal, "A Nyquist Rate Pixel Level ADC for CMOS Image Sensors, *IEEE Journal of Solid State Circuits,* **34**, 348-356, 1999.